



## **Episodic outbreaks bias estimates of age-specific force of infection: a corrected method using measles as an example.**

Authors	Ferrari, M J; Djibo, A; Grais, RF; Grenfell, B T; Bjørnstad, O N
Citation	Episodic outbreaks bias estimates of age-specific force of infection: a corrected method using measles as an example. 2010, 138 (1):108-16 Epidemiol. Infect.
DOI	<a href="https://doi.org/10.1017/S0950268809990173">10.1017/S0950268809990173</a>
Publisher	Cambridge University Press
Journal	Epidemiology and Infection
Rights	Archived with thanks to Epidemiology and Infection and Cambridge University Press
Download date	03/10/2021 17:17:46
Link to Item	<a href="http://hdl.handle.net/10144/98914">http://hdl.handle.net/10144/98914</a>

# Episodic outbreaks bias estimates of age-specific force of infection: a corrected method using measles as an example

M. J. FERRARI<sup>1,2\*</sup>, A. DJIBO<sup>3</sup>, R. F. GRAIS<sup>4</sup>, B. T. GRENFELL<sup>1,2</sup>  
AND O. N. BJØRNSTAD<sup>1,2,5</sup>

<sup>1</sup> Center for Infectious Disease Dynamics, Penn State University, PA, USA

<sup>2</sup> Department of Biology, Penn State University, PA, USA

<sup>3</sup> Ministry of Health, Niger

<sup>4</sup> Epicentre, France

<sup>5</sup> Department of Entomology, Penn State University, PA, USA

(Accepted 15 May 2009)

## SUMMARY

Understanding age-specific differences in infection rates can be important in predicting the magnitude of and mortality in outbreaks and targeting age groups for vaccination programmes. Standard methods to estimate age-specific rates assume that the age-specific force of infection is constant in time. However, this assumption may easily be violated in the face of a highly variable outbreak history, as recently observed for acute immunizing infections like measles, in strongly seasonal settings. Here we investigate the biases that result from ignoring such fluctuations in incidence and present a correction based on the epidemic history. We apply the method to data from a measles outbreak in Niamey, Niger and show that, despite a bimodal age distribution of cases, the estimated age-specific force of infection is unimodal and concentrated in young children (<5 years) consistent with previous analyses of age-specific rates in the region.

**Key words:** Age structure, estimation, force of infection, measles (rubeola).

## INTRODUCTION

The global reduction in the burden of measles through vaccination is one of the great milestones of public health [1, 2]. However, despite an estimated 60% reduction in measles mortality worldwide since 1999, measles remains a leading cause of vaccine-preventable death in children aged <5 years in sub-Saharan Africa [2]. Measles is classically an infection of children as infection conveys lifelong immunity preventing re-infection in older individuals. In the

pre-vaccine era, measles was primarily concentrated in school-aged children in the industrialized world [3]. Developing countries tend to be characterized by an even lower mean age at infection, which is important as disease severity and case-fatality rates are higher in younger children [4–6].

Understanding age-specific differences in infection rates is important in predicting the magnitude and mortality of outbreaks and identifying core age groups for vaccination programmes. The age-specific force of infection (FOI), defined as the age-specific rate at which susceptible individuals contract infection, can be studied mathematically using the catalytic model [7, 8]. The catalytic model defines how to discount the observed age distribution of cases by the predicted accumulation of immunity with age. The standard

\* Author for correspondence: Dr M. J. Ferrari, Center for Infectious Disease Dynamics, Department of Biology, 208 Mueller Laboratory, Penn State University, University Park, PA 16802, USA.  
(Email: mferrari@psu.edu)

catalytic model assumes that the age-specific FOI is constant through time, corresponding to the temporal equilibrium of dynamic epidemiological models. However, this assumption, may often be violated in the face of cyclical variation in incidence [5, 7–9] as is common for many acute, immunizing infections, like measles, that tend to show annual or multi-annual cycles [10–13].

At the extreme of outbreak irregularity, Ferrari *et al.* [13] recently showed that measles dynamics in Niamey, the capital of Niger, are characterized by frequent local extinction and episodic outbreaks that can vary over many orders of magnitude. These patterns result from the interplay between strong seasonality in transmission rates and very high birth rates. Such patterns of outbreaks violate the key assumption of the catalytic model. Catalytic models have generally not been assessed for the impact of fluctuating dynamics; although pulses of immunity through mass vaccination have been studied [14]. As an exception, Whitaker & Farrington [9], found that seasonal fluctuations in incidence had minimal impact on estimates of age-specific FOI; however, it is not clear how these important findings extend to the highly irregular multi-annual outbreak dynamics in Niamey. Here we address this issue, presenting an analysis of the age-specific FOI in Niamey from incidence data collected during the outbreak in 2003–2004. We describe the biases introduced by the episodic pattern of outbreaks and present a correction to the catalytic model that allows estimation of the age-specific FOI under episodic or periodic outbreak dynamics.

## METHODS

The catalytic model estimates the age-specific FOI of immunizing pathogens by recognizing that the probability of infection at any given age,  $a$ , is the joint probability of infection at age  $a$  and the probability of not having been infected in the interval 0 to  $a - 1$ . Note that while we consider discrete age groups corresponding to the relevant age-specific heterogeneities (and data reporting), the extension to continuous age structure is trivial. If  $\Phi(a)$  is the age-specific FOI, then the probability of infection at age  $a$ ,  $P(a)$ , is:

$$P(a) = \exp\left(-\sum_{t=0}^{a-1} \Phi(t)\right) (1 - \exp(-\Phi(a))), \quad (1)$$

for age groups of equal length.

Estimating the absolute age-specific FOI  $\Phi(a)$  from age-stratified case-notification data is possible only if the number of susceptibles (i.e. the denominator) is known [7, 8, 15]. However, in the absence of data on the susceptible population, estimates of the FOI can be made using cumulative seroprevalence as a measure of ‘those exposed’ [15]. We show below, using simulated data, that we can extend this approach to estimate the relative age-specific FOI, up to an unknown constant by using the total case reports as the denominator (see Results – Simulated data section below). Assuming that the incidence of infection is constant through time and the age distribution is uniform, and denoting the number of cases in age group  $a$  by  $I_a$  we can then model the vector  $\mathbf{I}$  as a draw from a multinomial distribution with probability vector  $\theta$  that represents a scaled version of the probability of infection-at-age according to:

$$\theta(a) = \frac{P(a)}{\sum_{i=1}^a P(i)}. \quad (2)$$

If the age distribution is not uniform within the age-range relevant for the infection in question, as is the case in many developing countries because of the high childhood mortality, we can further to re-scale  $\theta$  by the age pyramid (subject to the constraint  $\sum \theta(a) = 1$ ) to reflect the lower probability of observing cases in older age groups because the denominator decreases over and above the decrease due to the accumulation of immunity [14]. Combining models (1) and (2) with a multinomial likelihood, we can estimate the relative age specific FOI from case-at-age data using standard maximum-likelihood or Bayesian methods.

As discussed above, the catalytic model assumes that the probability of infection at a particular age is constant over time. However,  $\Phi(a, t)$  can in general be written as

$$\Phi(a, t) = \int_{d'=1}^A \beta(a, d') I(d', t) dd',$$

where  $\beta(a, d')$  is the transmission rate from age group  $a$  to  $d'$  and  $I(d', t)$  is the number of infected individuals, of age  $d'$ , at time  $t$  [9], which makes explicit the dependence of the FOI on the time-specific incidence of infection. The standard catalytic model requires that the incidence of infection through time is roughly constant at some average incidence,  $\bar{I}$ . In the face of the variable incidence that results from cyclic or erratic outbreaks, this assumption will be violated.

While this is a strong assumption, the consequences of its violation may not be too severe if the incidence-at-age data are collected over a long period relative to the frequency of the outbreaks [9]. However, as we show below, severe biases can result if the data are cross-sectional or collected during any given major outbreak.

In general, long-term disease incidence data are reported as the total over all age groups (see the example for Niamey below). As such, we make the simplifying assumption that  $\Phi(a, t)$  can be written as

$$\Phi(a, t) = \beta(a)I(t),$$

where,  $\beta(a)$  is the rate of infection of age group  $a$  from all other age groups, and  $I(t)$  is the total incidence at time  $t$ . This is equivalent to assuming the equilibrium age distribution of infected individuals through time. While this assumption ignores potential variation in the age distribution of disease incidence through time (see below), which is often unknown, it represents an improvement over the classic methods, as we show below, by accounting for time-varying incidence, which often is known.

The irregular, episodic outbreaks that result from the strong seasonal forcing and high birth rates result in strong violations of the assumption of time-invariance of the age-specific FOI. For example, a 4-year-old child in an epidemic year will experience a much higher probability of infection than a 4-year-old child in a non-epidemic year. To correct for this, we need to weight the probability of infection at age  $a$  in model (1) by the incidence of infection at age  $a$ . To make the assumption of constant incidence explicit, we re-write model (1) as:

$$P(a) = \exp\left(-\sum_{t=0}^{a-1} \beta(t)\bar{I}\right) (1 - \exp(-\beta(a)\bar{I})), \quad (3)$$

Accounting for the variable epidemic history, we can rewrite model (3) according to:

$$P(a) = \exp\left(-\sum_{t=0}^{a-1} \beta(t)I(t-a)\right) (1 - \exp(-\beta(a)I(0))), \quad (4)$$

where  $I(t-a)$  indicates the incidence  $a$  time steps prior to that of the time in question. Thus, the age-specific probability of being susceptible just prior to the time of the sample [the first term in model (4)] is the age-specific transmission rate weighted by the history of exposure of each age group. For our

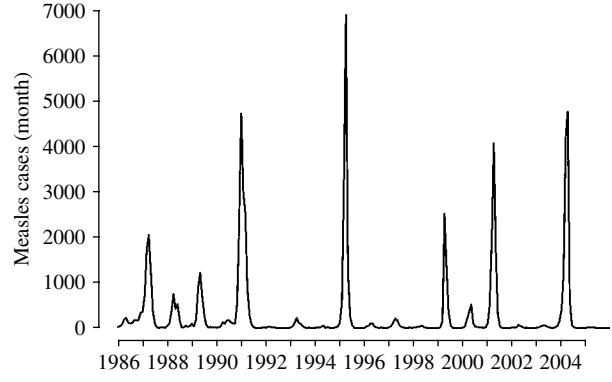


**Fig. 1.** Monthly incidence of measles cases in Niamey, Niger, 1986–2005.

modified method, we re-write model (4) as,

$$\begin{aligned} P(a) &= \exp\left(-\sum_{t=0}^{a-1} \frac{I(t-a)}{\bar{I}} \beta(t)\bar{I}\right) \left(1 - \exp\left(-\frac{I(0)}{\bar{I}} \beta(a)\bar{I}\right)\right) \\ &= \exp\left(-\sum_{t=0}^{a-1} \frac{I(t-a)}{\bar{I}} \Phi(t)\right) \left(1 - \exp\left(-\frac{I(0)}{\bar{I}} \Phi(a)\right)\right) \end{aligned} \quad (5)$$

which is the original catalytic model (1) corrected by the scaled epidemic history,  $I(t)/\bar{I}$ . Note that as incidence becomes less variable model (5) collapses to the original catalytic model (1).

## DATA

### The 2003–2004 outbreak of measles in Niamey, Niger

Niamey is a city of about 800 000 people in south-western Niger. Measles is regionally endemic in Niger, but dynamics within Niamey are characterized by outbreaks during the dry season (November–June) sometimes followed by local extinction [13]. Because of the episodic outbreaks, incidence can vary by several orders of magnitude from year to year (e.g. there were 85 cases reported in 1992 vs. 12302 cases in 1995), with deep troughs and long gaps between epidemics (Fig. 1). The actual probability of infection-at-age can therefore vary greatly from year to year.

A large outbreak of measles in Niamey occurred from November 2003 to July 2004. Case records from 11073 individuals reported to health centres ‘Centres de Santé Intégrés’ (CSI) and hospitals were collected retrospectively (from 1 November 2003 to 20 April 2004) and prospectively (from 21 April to 6 July 2004) by Epicentre in conjunction with the

Ministry of Health of Niger, the World Health Organization, and Médecins Sans Frontières. The WHO clinical case definition was used. At the beginning of the outbreak, ten cases were laboratory confirmed through detection of measles-specific IgM antibodies by the Ministry of Health. Of these records, the patient's age (in months), sex, date of symptom onset, vaccination status, and *quartier* (neighbourhood) of origin were recorded for 7689 cases. In addition to the detailed data from the 2003–2004 outbreak, the Ministry of Health has monitored monthly measles incidence for the city of Niamey since 1986 (Fig. 1).

While the ages of patients were recorded in 1-month intervals during the 2003–2004 outbreak, we aggregated the data into 6-month age groups from ages 0 to 20 years to account for uncertainty in true ages; the raw data had disproportionately many children reported to be of age exactly 12, 24, 36, 48, and 60 months. For our analyses, we randomly assigned these individuals into the age group above or below with an even probability. The population age structure was assumed to be pyramidal to account for high rates of mortality. The size of age group  $a$ ,  $N(a)$ , was assumed to follow the relationship  $N(a) = N(0) \exp(-0.0045a)$ , for  $a = 0, \dots, 20$ , which agrees well with the published age pyramid for Niger [16].

To correct the FOI estimates according to model (3) we aggregated the monthly 1986–2004 incidence time-series into 6-month time steps. Thus, an individual who was aged between 4 and 4.5 years during the 2003–2004 outbreak would have experienced an epidemic history of 149 cases during the 0–0.5 year age group, eight cases during the 0.5–1 year age group, 195 cases during the 1–1.5 years age group, etc. (see Fig. 1).

We fitted the relative age-specific FOI as a piecewise constant function (i.e. separate estimates for each age group with no explicit parametric form). We estimated the parameters using a Bayesian framework. The joint posterior distribution of the age-specific FOI was calculated using a Markov chain Monte Carlo implemented in the statistical software package R [17]. We ran the chain for 50 000 iterations after a burn-in period of 10 000 iterations and sampled every 100th iteration to avoid autocorrelation in the chain. We chose non-informative gamma priors for the FOI in each age group. Point estimates are given as the mean of the posterior distribution and 95% credible intervals are the 2.5th and 97.5th percentiles of the posterior distribution.

## Simulation

To evaluate if and how the estimates of age-specific FOI from the standard catalytic model may be biased because of episodic outbreaks, we generated data from a stochastic, age-structured, seasonally forced dynamic SIR-type model. The birth rate was taken to be to 50.71/1000 as reported for Niamey [16]. We chose sinusoidal forcing on the seasonal transmission rate according to:  $\beta(t) = \beta_0(1 + \beta_1 \cos(2\pi t/365))$ . We set  $\beta_0 = 5.5 \times 10^{-5}$ , the mean transmission rate for Niamey [13], and set  $\beta_1 = 0.8$ , which produces episodic dynamics in the chaotic regime, consistent with that observed for Niamey from 1986 to 2004 [13]. The population was structured into 41 age groups representing 6-month intervals from 0–20 years of age plus an additional category representing individuals > 20 years of age. We simulated the model in discrete, daily time steps. The number of new infected cases in age group  $a$  at time step  $t$ ,  $Y_{a,t}$ , was assumed to be a Poisson random variable with expected value

$$E[Y_{a,t}] = \beta_{t-1} \mathbf{B}_a \mathbf{I}_{t-1} S_{a,t-1},$$

where  $\mathbf{I}_{t-1}$  is an  $a \times 1$  vector representing the number of infected individuals in each age group at time  $t-1$  and  $\mathbf{B}_a$  is the  $a$ th row of the mixing matrix indicating the relative mixing rates in age groups [14, 18]. We chose  $\mathbf{B}$  to have the structure

$$\mathbf{B} = \begin{pmatrix} B_1 & B_2 & \dots & B_{21} \\ B_2 & B_2 & \dots & B_{21} \\ \vdots & \vdots & \ddots & B_{21} \\ B_{21} & B_{21} & B_{21} & B_{21} \end{pmatrix},$$

where  $B_i$  is proportional to the relative age-specific FOI for age group  $i$  estimated for the 2003–2004 Niamey outbreak (see below). The form of the mixing matrix implies that mixing is non-assortative and individuals mix equally with all younger age groups, as might be the case in settings such as Niger where younger siblings are minded by older siblings in extended family groups [19]. Sensitivity of the results to the explicit form of the mixing matrix is small for reasonable structures (see Supplementary Fig. 1, available in the online version of the paper).

We simulated epidemic dynamics for 30 years and applied models (3) and (5) to estimate the relative age-specific FOI from the epidemic in the 30th year provided the number of cases in that year was > 300. We replicated this for 200 simulated time-series with and without using the 20-year epidemic history to correct the estimate.

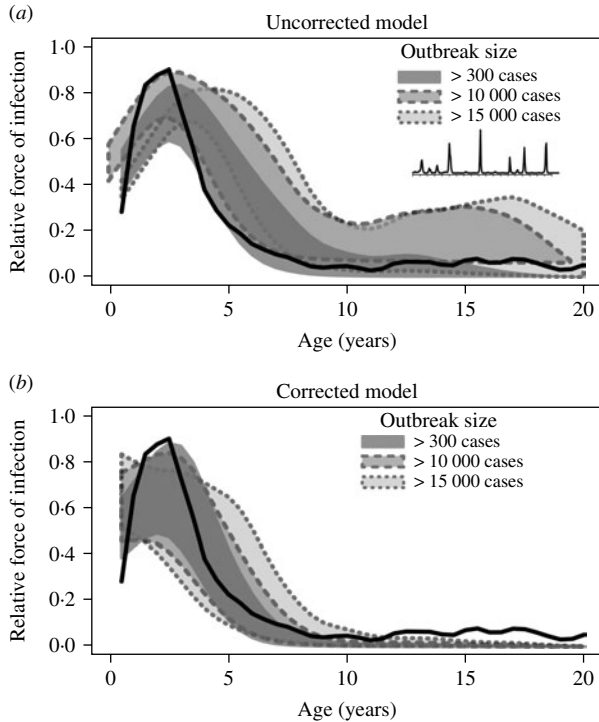


**Fig. 2.** Distribution of estimates of relative age-specific force of infection (FOI) for simulated episodic time-series. For each simulation, the FOI is scaled to have a maximum at 1 for presentation. Shaded regions give the central 50% of estimates for outbreaks of size  $> 300$  (solid lines,  $n=416$  epidemics),  $> 10\,000$  (dashed lines,  $n=99$ ), and  $> 15\,000$  (dotted lines,  $n=37$ ). The solid line indicates true relative age-specific FOI for the simulation. (a) Estimates assuming constant incidence history, (b) estimates corrected using the epidemic history.

## RESULTS

### Simulated data: bias due to irregular epidemic history

Both the standard catalytic approach and the corrected model work well for regular annual and biennial dynamics with small epidemic peaks (see Supplementary Figs 2 and 3, available online). For more strongly seasonal dynamics, which give erratic outbreaks, the two methods begin to diverge. Both methods give similar mean estimates of the relative age-specific FOI that appear unbiased for the true FOI (Fig. 2; outbreaks  $> 300$  cases), consistent with the analysis of Whitaker & Farrington [9]. However, for more erratic dynamics the estimates of the uncorrected model can be much more variable, especially in the older age groups (Fig. 2). This variability arises from the bias in the standard catalytic model when applied to large outbreaks. The episodic dynamics similar to those observed in Niamey can produce

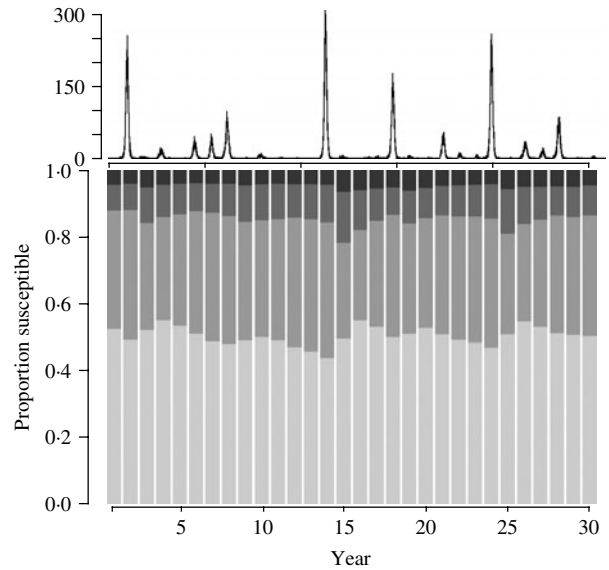


**Fig. 3.** Age distribution of susceptible individuals for a characteristic simulation of the age-structured model. Shaded bars indicate the proportion of the susceptible population in age groups 0–2 years,  $> 2$ –6 years,  $> 6$ –10 years,  $> 10$  years (dark to light shading respectively). Top panel shows the time-series of cases for the simulated data.

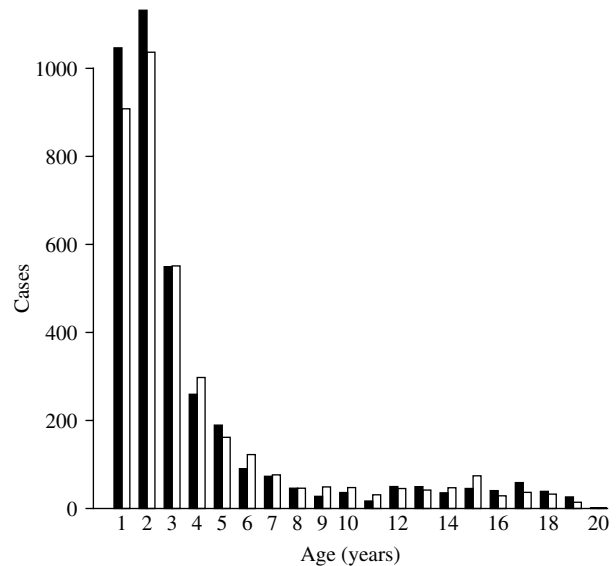


**Fig. 4.** Age distribution of measles cases reported in Niamey, Niger between 1 November, 2003 and 20 June 2004. ■, Male cases; □, female cases.

outbreaks ranging over several orders of magnitude. When applied to these large outbreaks (of the size of the Niamey 2003–2004 outbreak:  $\sim 11\,000$  reported cases), the standard catalytic model has a strong positive bias in the age-specific FOI for older

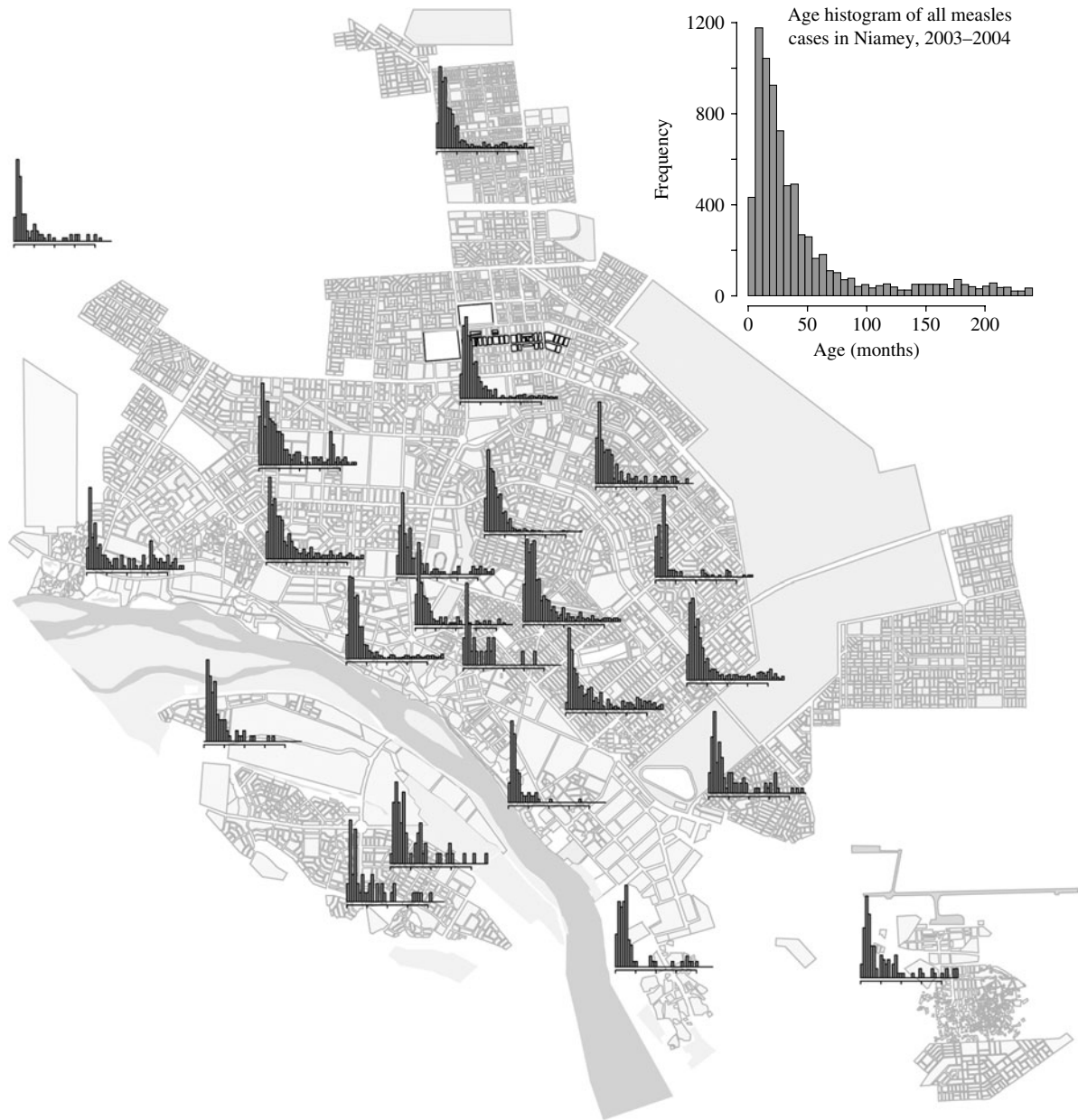


**Fig. 5.** Age distribution of measles cases in health centre districts in the 2003–2004 outbreak. Inset gives age distribution for all of Niamey.

age groups. Further, the age-at-peak FOI is overestimated for large outbreaks. The magnitude of the bias scales with the size of the outbreak; a slight positive bias for outbreaks  $>10\,000$  cases and a stronger bias with the appearance of a second mode at  $\sim 15$  years for outbreaks  $>15\,000$  cases (Fig. 2*a*). Thus, ignoring the time-varying FOI due to variable incidence leads to an overestimate of the transmission in older age group individuals for case-at-age data collected during large outbreaks (as is the case for the Niamey 2003–2004 outbreak data below). In contrast,

the corrected model more accurately recovers the shape of the age-specific FOI for both small and large outbreaks (Fig. 2*b*). In particular, the corrected model is not overtly biased for older age groups. However, while the age-of-peak FOI is well estimated for outbreaks up to 15 000 cases, there is a slight negative bias in the peak age for the largest epidemics (Fig. 2*b*).

The source of the bias in the older age groups, when using the standard catalytic model, can be understood by considering the changing age distribution of

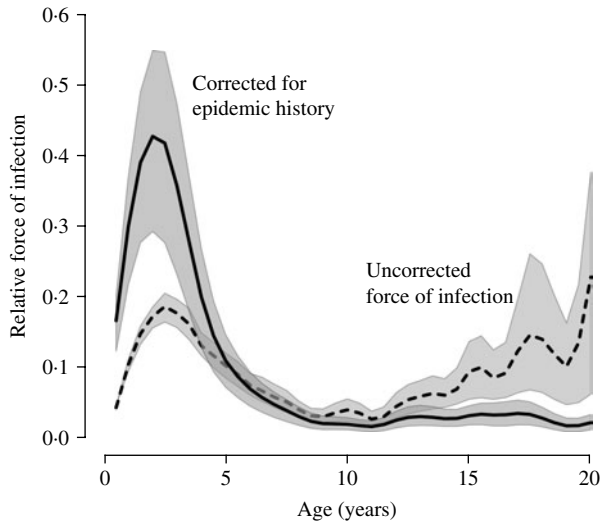


**Fig. 6.** Estimates the relative age-specific force of infection (FOI) in Niamey, Niger for the 2003–2004 outbreak. The dashed curve gives the smoothed mean of the posterior distribution for the FOI at each age group estimated using the catalytic model. The solid curve gives the smoothed mean of the posterior for the catalytic model corrected for the epidemic history. Grey shading gives the 95% credible intervals for each.

susceptibles through time (Fig. 3). In the intervals between major outbreaks, susceptibles accumulate in the later age groups due to the lower overall FOI, despite their being in relatively high-risk age groups. The susceptibles that are outside the high-risk age groups experience a lower overall age-specific FOI and are thus less likely to become infected in small to moderate epidemics. As such, the older age groups become relatively over-represented in the large epidemics compared to the situation in which incidence is constant across years.

#### Real data: the 2003–2004 outbreak in Niamey

The age distribution of cases during the 2003–2004 outbreak in Niamey was strongly right skewed (Fig. 4): the mean and median ages are 4.31 and 2.25 years, respectively. Despite the strong concentration of cases in young children, the tail of the distribution is heavy, with a second minor mode at around age 15 years. While small in number, the incidence in older age groups is surprising as these individuals would be expected to have contracted measles earlier in life and thus be immune.

The age distribution of cases in males and females did not differ (Fig. 4). There was no spatial pattern in the age distribution of cases within the city (Fig. 5).

Thus, the long tail of the age distribution does not appear to be associated with gender-specific or geographic heterogeneities.

We fitted the relative age-specific FOI to the 2003–2004 incidence data using the classic catalytic model (3), and the corrected model (4). Fitting the FOI using the classic model suggests that there is a bimodal age-specific FOI with a peak at 2.5–3 years followed by an increase from ages 10–20 years (Fig. 6). Our corrected model that accounts for the epidemic history yields a unimodal estimate with a peak at age 2.5–3 years that subsequently declines more or less monotonically with age (Fig. 6).

## DISCUSSION

Understanding the age-specific dynamics of disease transmission is important for calibrating models [20, 21] and effectively planning age-targeted vaccination strategies [22]. In a very important contribution, Whitaker & Farrington [9] showed that, despite the implicit assumption of endemic equilibrium, regular cyclic epidemic dynamics do not strongly bias the standard catalytic model. In areas with strong seasonal variation in transmission and high birth rates, regular epidemic cycles can break down and give rise to erratic outbreaks that vary strongly in magnitude [13]. Here we have shown that erratic outbreak dynamics lead to systematic biases in the estimation of the age-specific FOI for large outbreaks when using the standard catalytic model, resulting in an overestimate of the role of older individuals. Further, we have presented a method to correct the age-specific FOI estimates using the previous epidemic history.

Measles outbreaks in Niamey can vary greatly from year to year as a consequence of strong seasonal forcing, high birth rates, and stochastic re-introduction following local extinction [13]. In the face of this variability, the classical methods to analyse age-specific incidence data lead to biased estimates of the age-specific FOI. Indeed, the classic, uncorrected catalytic model predicts an unusually high FOI in the 10–20 years age groups. Measles is classically thought of as a childhood disease, and an increasing FOI in older age groups is inconsistent with prior observations, at low to medium vaccination rates, in both industrialized [3, 15] and developing countries [4–6]. Our modified method that accounts for the epidemic history shows that the observed age distribution of measles cases in the 2003–2004 outbreak is consistent



with high FOI in young children, and is consistent with childhood transmission as observed elsewhere [4–6]. The apparently high FOI in older age groups that was estimated by the standard model can be explained parsimoniously as a spurious result of the erratic but recurrent epidemics.

There are alternative explanations for the observed age distribution of cases in Niamey. The high incidence of older cases could be the result of higher reporting rates in older age groups. However, measles tends to be more severe in younger children [23, 24]; and previous studies of the age-specific reporting rate have suggested that reporting in older age groups tends to be lower rather than higher [6]. Alternatively, the older cases may represent immigrants from regions with relatively low measles exposure, or increased exposure in older age groups due to childcare (of offspring or siblings). However, both of these hypotheses, require the supposition of mechanisms for which there is no empirical support. Further, the observed similarity of the male and female age distributions does not suggest any sex bias in the age distribution as might be expected if childcare or migration were strong drivers of the observed pattern. Thus, the most parsimonious explanation of the observed age distribution of cases is the interaction between erratic dynamics and age-structured transmission.

While estimating the absolute age-specific FOI is ideal for developing age-structured models of epidemic dynamics, it is often difficult in the absence of data about the size of the susceptible population. The methods we have presented illustrate that we can use case-at-age data to estimate the *relative* age-specific FOI, which allows us to understand the relative contributions of age groups to epidemic dynamics and inform age-specific policy recommendations.

The public health consequence of our calculations is that age-targeted vaccination programmes in Niamey should continue to focus on young children, where the bulk of the FOI is concentrated. It further argues strongly for the continuation of follow-up strategies, such as catch-up campaigns, to reduce the accumulation of susceptible individuals in older age groups during the intervals between outbreaks. These individuals may themselves reside in relatively low-risk age groups, yet they may provide fuel to sustain the chains of transmission during the major outbreaks. Further, the accumulation of older-aged women without prior exposure to measles means more children will be born without maternal immunity to

measles. In the 2003–2004 Niamey outbreak 206 cases (2·6%) were aged <6 months and 850 cases (11·1%) were aged <9 months. Given the high case fatality in very young children [22], the reduction of maternal immunity due to the accumulation of susceptible women in older age groups could have disproportionate effects on the overall burden of measles mortality in the future.

A corollary to these observations is the insight that the age structure of cases should be expected to be constant across outbreaks of different magnitudes. This is particularly important in highly seasonal areas like Niger [13], but may become increasingly relevant as vaccine uptake increases in less seasonally forced areas and outbreaks become less regular [25]. As a result, calculations of the burden of measles mortality and morbidity that rely on the assumption of static age distributions (e.g. [2, 26]) may result in biased estimates of measles burden.

## ACKNOWLEDGEMENTS

We thank the reviewers whose comments greatly contributed to the improving of this work. We acknowledge the support of the Niger Ministry of Health and Médecins Sans Frontières for access to the data on the Niamey outbreak. M.F., B.G. and O.B. were funded by the RAPIDD programme of the Science & Technology Directorate, Department of Homeland Security, and the Fogarty International Center, National Institutes of Health and a grant from the Bill and Melinda Gates Foundation. B.G. was additionally funded by the National Institutes of Health (R01 GM083983-01).

## NOTE

Supplementary material accompanies this paper on the Journal's website (<http://journals.cambridge.org/hyg>).

## DECLARATION OF INTEREST

None.

## REFERENCES

1. Cliff AD, Haggett P, Smallman-Raynor M. *Measles: An Historical Geography of a Major Human Viral Disease from Global Expansion to Local Retreat, 1840–1990*. Oxford: Blackwell, 1993, pp. 462.

2. **Wolfson LJ, et al.** Has the 2005 measles mortality reduction goal been achieved? A natural history modelling study. *Lancet* 2007; **369**: 191–200.
3. **Edmunds WJ, et al.** The pre-vaccination epidemiology of measles, mumps and rubella in Europe: implications for modelling studies. *Epidemiology and Infection* 2000; **125**: 635–650.
4. **Enquselassie F, et al.** Seroepidemiology of measles in Addis Ababa, Ethiopia: implications for control through vaccination. *Epidemiology and Infection* 2003; **130**: 507–519.
5. **Remme J, Mandara MP, Leeuwenburg J.** The force of measles infection in East Africa. *International Journal of Epidemiology* 1984; **13**: 332–339.
6. **Scott S, et al.** Estimating the force of measles virus infection from hospitalised cases in Lusaka, Zambia. *Vaccine* 2004; **23**: 732–738.
7. **Griffiths DA.** A catalytic model of infection form measles. *Applied Statistics* 1974; **23**: 330–339.
8. **Muench H.** *Catalytic Models in Epidemiology*. Cambridge, MA: Harvard University Press, 1959, pp. 110.
9. **Whitaker HJ, Farrington CP.** Estimation of infectious disease parameters from serological survey data: the impact of regular epidemics. *Statistics in Medicine* 2004; **23**: 2429–2443.
10. **Fine PEM, Clarkson JA.** Measles in England and Wales. 1. An analysis of factors underlying seasonal patterns. *International Journal of Epidemiology* 1982; **11**: 5–14.
11. **Grenfell BT, Bjornstad ON, Kappey J.** Travelling waves and spatial hierarchies in measles epidemics. *Nature* 2001; **414**: 716–723.
12. **Schaffer WM, Kot M.** Nearly one dimensional dynamics in an epidemic. *Journal of Theoretical Biology* 1985; **112**: 403–427.
13. **Ferrari MJ, et al.** The dynamics of measles in sub-Saharan Africa. *Nature* 2008; **451**: 679–684.
14. **Anderson RM, May RM.** *Infectious Diseases of Humans: Dynamics and Control*. Oxford: Oxford University Press, 1991, pp. 768.
15. **Grenfell BT, Anderson RM.** The estimation of age-related rates of infection from case notifications and serological data. *Journal of Hygiene* 1985; **95**: 419–436.
16. **CIA.** World Factbook: Niger. Central Intelligence Agency, USA, 2007.
17. **Gilks W, Richardson S, Spiegelhalter DJ.** *Markov Chain Monte Carlo in Practice*. London: Chapman & Hall, 1996, pp. 486.
18. **Kanaan MN, Farrington CPA.** Matrix models for childhood infections: a Bayesian approach with applications to rubella and mumps. *Epidemiology and Infection* 2005; **133**: 1009–1021.
19. **Goddard AD.** Changing family structures among rural Hausa. *Africa* 1973; **43**: 207–218.
20. **Schenzle D.** An age-structured model of pre- and post-vaccination measles transmission. *IMA Journal of Mathematics Applied in Medicine and Biology* 1984; **1**: 169–191.
21. **Bolker BM, Grenfell BT.** Chaos and biological complexity in measles dynamics. *Proceedings of the Royal Society of London, Series B: Biological Sciences* 1993; **251**: 75–81.
22. **Grais RF, et al.** Unacceptably high mortality related to measles epidemics in Niger, Nigeria, and Chad. *PLOS Medicine* 2007; **4**: 122–129.
23. **Burstrom B, Aaby P, Mutie DM.** Measles in infants – a review of studies on incidence, vaccine efficacy and mortality in East Africa. *East African Medical Journal* 1995; **72**: 155–161.
24. **Kambarami RA, et al.** Measles epidemic in Harare, Zimbabwe, despite high measles immunization coverage rates. *Bulletin of the World Health Organization* 1991; **69**: 213–219.
25. **Earn DJD, et al.** A simple model for complex dynamical transitions in epidemics. *Science* 2000; **287**: 667–670.
26. **Stein CE, et al.** The global burden of measles in the year 2000 – a model that uses country-specific indicators. *Journal of Infectious Diseases* 2003; **187**: S8–S14.